

# Journal of Materials Chemistry C

Accepted Manuscript



This is an *Accepted Manuscript*, which has been through the Royal Society of Chemistry peer review process and has been accepted for publication.

*Accepted Manuscripts* are published online shortly after acceptance, before technical editing, formatting and proof reading. Using this free service, authors can make their results available to the community, in citable form, before we publish the edited article. We will replace this *Accepted Manuscript* with the edited and formatted *Advance Article* as soon as it is available.

You can find more information about *Accepted Manuscripts* in the [Information for Authors](#).

Please note that technical editing may introduce minor changes to the text and/or graphics, which may alter content. The journal's standard [Terms & Conditions](#) and the [Ethical guidelines](#) still apply. In no event shall the Royal Society of Chemistry be held responsible for any errors or omissions in this *Accepted Manuscript* or any consequences arising from the use of any information it contains.



## Ultrafast broadband optical limiting in simple pyrene-based molecules with high transmittance from visible to infrared regions

Zhengguo Xiao<sup>a</sup>, Yufang Shi<sup>b</sup>, Ru Sun<sup>c</sup>, Jianfeng Ge<sup>c</sup>, Zhongguo Li<sup>a</sup>, Yu Fang<sup>c</sup>, Xingzhi Wu<sup>a</sup>, Junyi Yang<sup>c</sup>, Minggen Zhao<sup>\*b</sup>, Yinglin Song<sup>\*a</sup>

Received 00th January 20xx,  
Accepted 00th January 20xx

DOI: 10.1039/x0xx00000x

www.rsc.org/

Pyrene is considered as one of the most promising nonlinear functional building blocks. The nonlinear optical properties of materials can be improved by modifying main nonlinear group possession ratio occupied in frontier molecular orbitals. Accordingly, we designed and synthesized two isomeric molecules based on pyrene for ultrafast broadband optical limiters. Different pyrene possession ratios occupied in frontier molecular orbitals were calculated through quantum chemical methods between two molecules. Higher average pyrene possession ratio occupied in frontier molecular orbitals exhibited better nonlinear properties in such structures, which was consistent with the experimental data. Excellent optical limiting behaviors were observed under femtosecond laser excitations at multi-wavelengths (range from 515 to 900 nm), which resulted from two-photon absorption (TPA) and TPA induced excited-state absorption (ESA). Moreover, the sample was extremely high transmittance (> 91%) from visible to infrared regions (500 to 900 nm). Our results show that pyrene-based derivatives can be considered as a promising candidate for broadband ultrafast optical limiters.

### 1. Introduction

Great efforts have been devoted to graphitic systems such as carbon black suspensions (CBS)<sup>1, 2</sup>, graphene families,<sup>3-5</sup> single-walled and multi-walled carbon nanotubes (CNT)<sup>6-8</sup> and  $\pi$ -electron conjugation systems such as fullerenes,<sup>9</sup> porphyrins and phthalocyanines<sup>10-13</sup> as optical limiting materials for protecting human eyes and sensitive optical sensors from laser damage. To gain ideal optical limiting apparatus, three factors should be taken into consideration: (i) high transmittance in low intensities and low transmittance in high intensities; (ii) fast response speed; (iii) broad spectral and temporal response characteristics. For graphene, CBS and CNT suspensions, their optical limiting properties are mainly caused by nonlinear scattering when solvent microbubbles and/or microplasmas are formed at high fluences as a consequence of energy transfer from the solute to the solvent.<sup>14-16</sup> However, the formation timescale of the microbubbles and microplasmas is about a few nanoseconds, which restrict the application in ultrafast laser field. Due to the large ratio of excited-state to ground-state absorption cross-section, the classical benchmark materials of fullerenes, porphyrins and phthalocyanines can also provide

prominent optical limiting properties. However, their poor optical transparent characteristics and narrow excited-state absorption (ESA) spectral regions hinder practical application in broadband optical limiter. So far, considerable papers have reported some materials possessed broad spectral optical limiting under nanosecond photoexcitation.<sup>3,17-26</sup> Especially, metal-based compounds are considered as new generation optical power limiting materials exhibiting highly transparent characteristic in the visible spectral region.<sup>27-30</sup> However, to our best of knowledge, only few papers reported the broad spectral nonlinear responses and broadband optical limiting behaviors under ultrafast photoexcitation.<sup>31-35</sup> Accompanied with the rapid development of ultrafast laser, it is essential to develop a broad spectral optical limiter for protecting eye and sensor from damage on ultrafast timescale.

Pyrene is considered as one of the most promising nonlinear functional building blocks. Some literatures have reported pyrene-based derivatives possessed large two-photon absorption cross section.<sup>36,37</sup> Moreover, pyrene-based derivatives possess abundant  $\pi$  electrons that are of extraordinary admirable optical transparent characteristics for visible and infrared regions. On the other hand, their nonlinear optical (NLO) properties can be improved by modifying main nonlinear group possession ratio occupied in frontier molecular orbitals. Accordingly, in this work, we designed and synthesized two isomeric pyrene derivatives **P1** and **P2** (Scheme 1) for ultrafast broadband optical limiters. Both of them are composed of pyrene, carbonyl, ethylene and thiophene groups. Apparently, the difference is the position of carbonyl group in these two molecules. Theoretically, the frontier molecular orbitals of **P1** and **P2** were calculated by quantum chemical methods.

<sup>a</sup> Harbin institute of technology, Harbin 150001, China  
E-mail: ylsong@hit.edu.cn

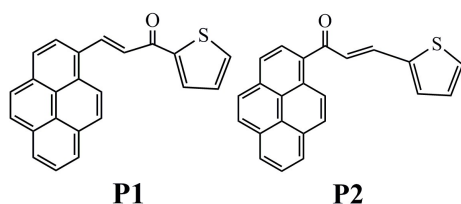
<sup>b</sup> Xinzhou Teacher's University, Xinzhou 034000, China  
\*E-mail: zhao\_minggen@aliyun.com

<sup>c</sup> Soochow University, Suzhou 215123, China

† Footnotes relating to the title and/or authors should appear here.

Electronic Supplementary Information (ESI) available: [details of any supplementary information available should be included here]. See DOI: 10.1039/x0xx00000x

Experimentally, we systematically investigated the broad spectrum nonlinear optical properties of **P1** and **P2** by performing broadband Z-scan measurements and transient absorption spectrum with 190 fs laser pulses.



Scheme 1. Chemical structures of **P1** and **P2**

## 2. Theoretical calculation and experimental methods

### 2.1 Synthetic procedures

#### Synthesis of 3-(pyren-1-yl)-1-(thiophen-2-yl)prop-2-en-1-one (**P1**):

The mixture of 1-pyrenecarboxaldehyde (230 mg, 1 mmol) and 40 mL dioxane was stirred until dissolved at room temperature. 2-acetyl thiophene (0.11 mL, 1 mmol) and 4 mL 10% of aqueous sodium hydroxide were sequentially added and the reaction system was heated at 50–60 °C. For 2 hours, the mixture was poured into ice water. The crude product was obtained by filtration and the final product (**P1**) was purified by recrystallization with acetone to afford compound **P1** (270 mg, 79%). M.P.: 170.0–172.0 °C. <sup>1</sup>H NMR (600 MHz, 298 K, DMSO-*d*<sub>6</sub>): δ = 8.89–8.84 (m, 2H), 8.66 (d, *J* = 9.6 Hz, 1H), 8.49 (d, *J* = 3.6 Hz, 1H), 8.42–8.37 (m, 4H), 8.32–8.26 (m, 2H), 8.23 (d, *J* = 15 Hz, 1H), 8.16–8.12 (m, 2H), 7.38 (t, *J* = 4.2 Hz, 1H). <sup>13</sup>C NMR (150 MHz, 298 K, DMSO-*d*<sub>6</sub>): δ = 181.53, 145.67, 138.81, 135.78, 133.94, 132.57, 130.87, 130.22, 129.74, 129.07, 128.98, 128.81, 128.02, 127.44, 126.74, 126.33, 126.09, 125.31, 125.07, 124.14, 123.97, 123.78, 122.36. MALDI-TOF (MS): Calc. for C<sub>23</sub>H<sub>14</sub>NaO<sup>+</sup>: [m/z + Na]<sup>+</sup> 361.06576, found: [m/z + Na]<sup>+</sup> 361.06591.

#### Synthesis of 1-(pyren-1-yl)-3-(thiophen-2-yl)prop-2-en-1-one (**P2**):

To a mixture of acetylpyrene (560 mg, 2 mmol) and 2-thiophene carboxaldehyde (2 mmol, 0.186 mL) in THF (50 mL), 10% of aqueous sodium hydroxide (3 mL) was added. The mixture was stirred and refluxed for 80 min, and yellow solid was formed. After filtration, the obtained power was washed with THF: H<sub>2</sub>O (v/v, 2:1) for three times to afford **P2** (510 mg, 75%). M.P. 148.0–149.0 °C. <sup>1</sup>H NMR (600 MHz, 298 K, DMSO-*d*<sub>6</sub>): δ = 8.57 (d, *J* = 9.0 Hz, 1H), 8.43–8.39 (m, 4H), 8.35–8.29 (m, 3H), 8.18 (t, <sup>1</sup>*J* = 7.8 Hz, <sup>2</sup>*J* = 7.2 Hz, 1H), 7.83–7.80 (m, 2H), 7.654 (d, *J* = 3.0 Hz, 1H), 7.37 (d, *J* = 9.6 Hz, 1H), 7.20 (t, <sup>1</sup>*J* = 4.8 Hz, <sup>2</sup>*J* = 3.6 Hz, 1H). <sup>13</sup>C NMR (150 MHz, 298 K, DMSO-*d*<sub>6</sub>): δ = 194.22, 139.44, 138.26, 133.35, 133.32, 132.73, 130.94, 130.70, 130.10, 129.16, 129.04, 128.87, 128.50, 127.28, 126.80, 126.47, 126.37, 126.05, 125.51, 124.52, 124.33, 123.99, 123.58. MALDI-TOF (MS): Calc. for C<sub>23</sub>H<sub>14</sub>NaO<sup>+</sup>: [m/z + Na]<sup>+</sup> 361.06576, found: [m/z + Na]<sup>+</sup> 361.06581.

### 2.2 Quantum chemical calculation

To improve the performance of materials for photonic applications, a fundamental knowledge of the relationship among chemical structure, electronic structure and NLO properties is required. It has been shown that the NLO properties of π-conjugated organic materials originated from the delocalization of the π-electron

cloud.<sup>38,39</sup> Hou et al.<sup>40</sup> investigated the effect of metal ions on the third-order nonlinear optical properties of metal-organic clusters by molecular orbital theory. Similarly, to investigate the contribution of substituent groups to NLO properties of **P1** and **P2**, we calculated its components of the frontier molecular orbital which corresponded to the delocalization of the π-electron cloud. The input structure data as for quantum chemical calculations of two molecules were provided in supplementary information file. The frontier molecular orbital distributions and energy levels were estimated by density functional theory (DFT) at the level of B3LYP/6-31+G\*\*//CPCM (DMSO) using the Gaussian 09 program package,<sup>41</sup> shown in Fig. 1. The possession percentage of each component occupied in frontier molecular orbitals was obtained by GaussSum<sup>42</sup> and summarized in Table 1. In general, the electron in HOMO or HOMO-1 is excited to LUMO or LUMO+1 after photoexcitation. When two-photon absorption (TPA) effect occurs, molecules absorb two photons, promoting electrons from HOMO-1, HOMO to LUMO, LUMO+1. These transition processes mainly occur at pyrene group because pyrene acts as the main electron donor in two molecules. Therefore, the main contribution to NLO properties should attribute to pyrene group. In molecule **P1**, the carbonyl group is close to thiophene and the conjugation system is mainly composed of pyrene and ethylene. As for **P2** molecule, the carbonyl group is close to pyrene group and thus the carbonyl group corresponds to electron withdrawing group. Different position of carbonyl group can give rise to different distribution of π-electron in pyrene group. Due to the presence of continuous carbonyl for **P2**, π-electron can transfer from pyrene group to carbonyl and ethylene group, which makes the average pyrene possession ratio of **P2** lower than that of **P1**. Compared with **P2**, **P1** has higher average pyrene possession ratio ((51%+41%+90%+95%)/4=69.25% for **P1** and (81%+18%+97%+2%)/4=49.5% for **P2**) occupied in frontier molecular orbitals, which indicates that **P1** possesses larger NLO responses than that of **P2**.

### 2.3 Z scan technique and optical limiting measurements

In femtosecond Z-scan measurements, the light source was used an optical parametric amplifier (OPA, Light Conversion ORPHEUS, 190 fs, 20 Hz) with the tunable wavelength ranging from 515 nm to 900 nm. The experimental apparatus was similar to that in Ref.<sup>43</sup>. The laser source used for fs-pulsed optical limiting measurements was the same as those used for open-aperture Z-scan technique and the sample was placed at the focus position in our Z-scan system. The repetition rate was also 20 Hz to eliminate spurious cumulative effects originated from thermally-induced nonlinearities. In the Z-scan measurement, the length of the sample is 2 mm, while in the optical limiting measurements, the length of the sample is 5 mm.

### 2.4 Transient absorption spectrum

The broadband transient absorption measurement was performed by use of femtosecond pulses generated by a regenerative amplified Yb: KGW fiber laser system (Light Conversion, PHAROS-SP) that produces 1 mJ pulses centered at 1030 nm with a repetition rate of 6 kHz and 190 fs (FWHM). The main part of fundamental output was delivered to pump an optical parametric amplifier (OPA, ORPHEUS, Light Conversion). The OPA output was tuned to 425 nm

wavelength as the pump beam, which were then modulated at 137 Hz using a chopper. The excitation pulses were attenuated to the desired intensity using a gradual neutral density optical filter for minimizing cross-phase modulation effects. Probe pulses for spectroscopic characterization were produced by passing a small portion of 1030 nm through a computer-controlled optical delay stage (with the maximum delay line of 1700 ps) and focusing into a

2 mm thick Ti: sapphire plate to produce a white-light continuum spanning the 478-780 nm window. The polarization of pump and probe pulses at the sample location was at magic angle to avoid anisotropic effect. The angle between pump and probe beams was 5° and the beam waist of pump and probe beam were nearly 1 mm and 100 μm in the sample solution, respectively.

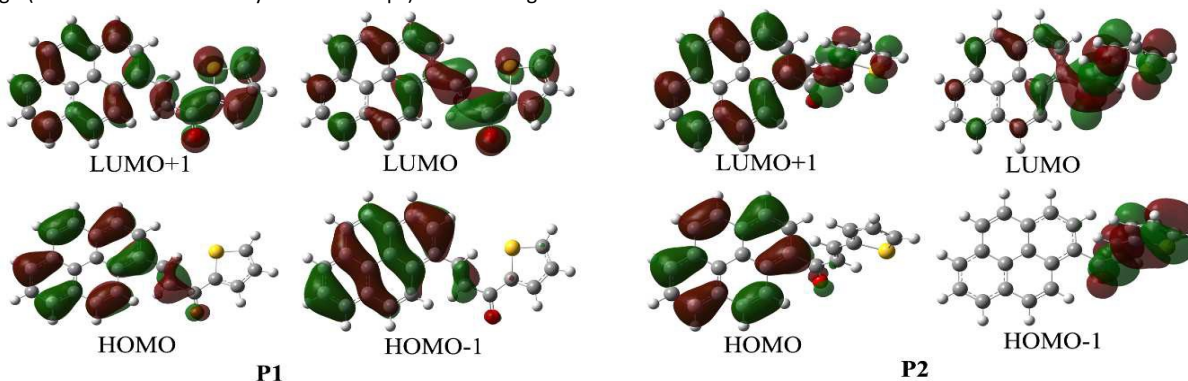


Fig. 1 The frontier molecular orbital distributions of **P1** and **P2** involved in the vertical excitation

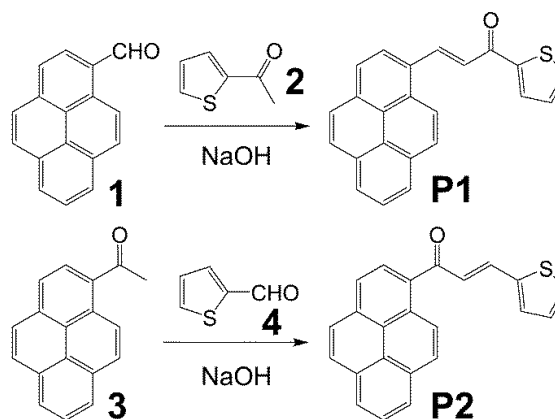
Table 1 The possession percentage of each component occupied in frontier molecular orbitals of **P1** and **P2**

	<b>P1</b>					<b>P2</b>				
	Energy	thiophene	pyrene	ethylene	carbonyl	Energy	thiophene	pyrene	ethylene	carbonyl
	/eV	/%	/%	/%	/%	/eV	/%	/%	/%	/%
LUMO+1	-1.98	29	51	5	15	-2.11	10	81	8	1
LUMO	-2.72	13	41	21	25	-2.68	28	18	26	28
HOMO	-5.81	1	90	7	2	-5.89	0	97	1	2
HOMO-1	-6.76	1	95	3	1	-6.79	61	2	27	10

### 3. Results and discussion

#### 3.1 Synthesis

The synthetic route to compounds **P1** and **P2** is outlined in Scheme 2. 1-Pyrenecarboxaldehyde (**1**) was treated with 2-acetylthiophene (**2**) in the presence of sodium hydroxide to produce compound **P1** in 79% yield. In the similar condition, compound **P2** was obtained as a yellow solid in 75% yield by condensation reaction between 1-acetylpyrene (**3**) and 2-thienaldehyde (**4**). These two new compounds were characterized by <sup>1</sup>H NMR, <sup>13</sup>C NMR and MALDI-TOF mass spectroscopies (See the supporting information Fig. S1 for <sup>1</sup>H NMR, Fig. S2 for <sup>13</sup>C NMR, Fig. S3 for MALDI-TOF mass spectroscopies). **P1** and **P2** were soluble in common polar solvents such as DMF and DMSO.



Scheme 2. Synthetic route to compounds **P1** and **P2**.

### 3.2 UV-visible absorption and fluorescence spectra

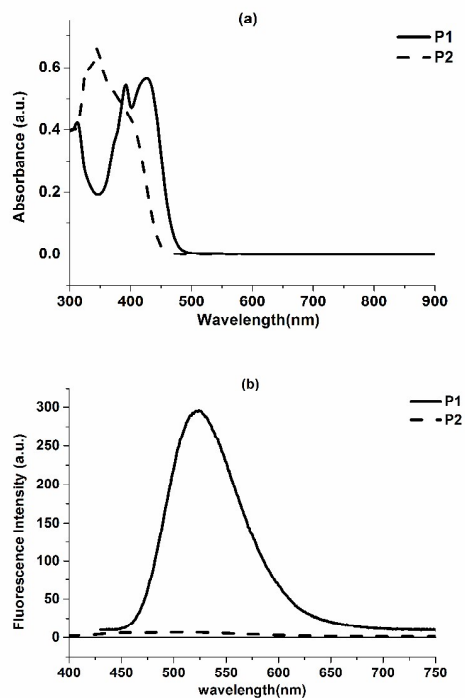


**Fig. 2** UV-vis absorption and emission spectra of compounds **P1** and **P2** in diluted dichloromethane solution.

The UV-Vis and emission spectra of compounds **P1** and **P2** were recorded in diluted dichloromethane at room temperature as shown in Fig. 2. **P1** and **P2** displayed the maximum absorption bands at 391 nm, 425 nm and 345 nm, respectively, which was assigned to the  $n-\pi^*$  and  $\pi-\pi^*$  transition. It should be noted that **P1** featured red-shift absorption compared with **P2**. This is because 3-(pyren-1-yl)acrylaldehyde part in **P1** presented larger conjugation length than pyrene or 3-(thiophen-2-yl)acrylaldehyde moieties in **P2**. When excited at the maximum absorption, **P1** performed strong fluorescent signal centered at 523 nm, while the fluorescent signal of **P2** is quenched by  $\pi$ -electron transfer from pyrene unit to conterminous carbonyl group.

### 3.3 open aperture Z-scan and transient absorption spectrum

To evaluate the nonlinear coefficients and have a good knowledge of the underlying mechanism for the observed optical nonlinearities, open-aperture Z-scan measurements were carried out at different levels of laser intensities  $I$  under different wavelengths femtosecond laser pulses. We conducted Z-scan experiments on the pure DMSO to exclude the optical nonlinearity originating from the solvent under identical experimental conditions. The concentration of both samples solution was 0.0137 mol/L. To study the NLO properties of two solutions, we first assumed that titled solution possessed only pure third-order optical nonlinearities and selected 600 nm open-aperture Z-scan measurements of **P1** solution as an example. All the Z-scan curves under different input intensities for 600 nm were shown in Fig. 3(b). Due to no peak or valley was observed for pure DMSO, the nonlinearity was only attributed to solute. By fitting to Z-scan theory,<sup>43</sup> we extracted the effective nonlinear absorption  $\beta_{\text{eff}}$ , at

different levels of  $I$ . From the Fig. 3(a), the measured  $\beta_{\text{eff}}$  was nearly proportional increasing function of input intensity  $I$ , suggesting that TPA was not the only mechanism and the occurrence of higher-order nonlinear absorption.

In fact, organic molecules such as charge-transfer salts may simultaneously exhibit both TPA and TPA induced ESA processes under photoexcitation.<sup>44, 45</sup> We supposed that the higher-order nonlinear absorption was the TPA induced ESA. To further confirm the assumption, femtosecond transient absorption spectrum was performed with 190 fs, pumped at 425 nm wavelength [see Fig. 4].

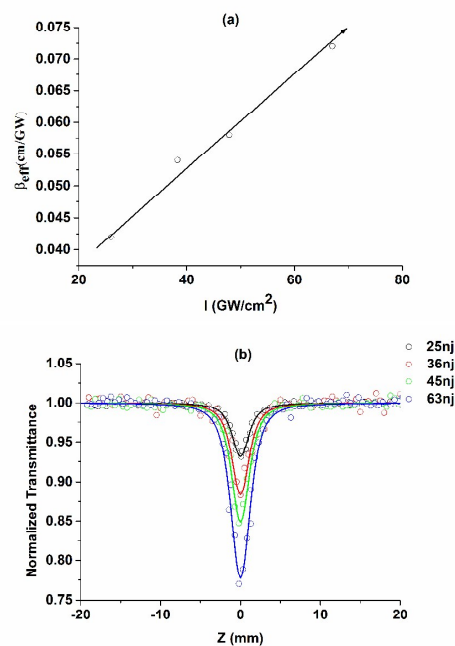


**Fig. 3** (a) Example of intensity dependence of nonlinear absorption coefficient for **P1** and (b) open-aperture Z-scan of **P1** at different energies of 25nj, 36nj, 45nj and 63nj under 600 nm, respectively.

The different colour circles are the experimental data and the corresponding colour solid lines represent the theoretical fitting.

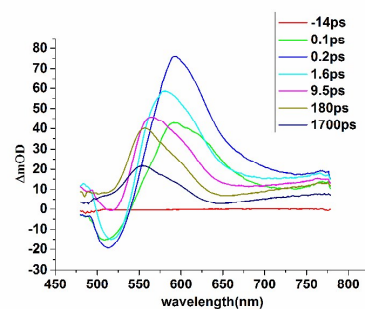


**Fig. 4** Transient absorption spectrum of **P1** pumped at 425 nm with 190 fs laser pulses

As can be seen, positive signal range from 550 to 780 nm appeared, which can be assigned to excited-state absorption (ESA).

The negative signal occurred within 9 picosecond centered at 520 nm wavelength correspond to stimulated emission from fluorescence spectra [Fig. 2(b)]. Under photoexcitation, molecules from the ground state  $S_0$  are excited to higher lying vibronic levels of  $S_1$ , then relax to the lowest vibronic level of  $S_1$  through vibrational cooling relaxation (VCR). Molecules undergoing ESA get excited to  $S_2$  instantaneously and decay back to  $S_1$ .

As for spectra regions between 495 nm and 540 nm, the absorption of this band is not accurately determined because of the contribution of stimulated emission (negative absorbance), which underlie the excited-state absorption signal (positive absorbance). To exclude the factor of fluorescence disturbance, we performed a degenerate pump-probe experiment at 532 nm (shown in Fig. S4, Supporting Information). The apparatus of pump-probe measurement was similar to reference.<sup>46</sup> From the Fig. S4, it was concluded that the sample experienced TPA firstly and then ESA. We also carried out a degenerate pump-probe experiment at 800 nm for limitation detection windows from 478 nm to 780 nm in transient absorption spectra (shown in Fig. S5, Supporting Information). It was implied that the nonlinear absorption was originated from TPA and TPA-assisted ESA at 800 nm. All the experiments were demonstrated the nonlinear absorption mechanism was TPA and TPA induced ESA.

Generally, TPA induced ESA can be considered as a fifth-order nonlinear absorption or effective three-photon absorption process.<sup>44, 47</sup> In the fitting procedures, we set the expression of absorption coefficient as  $\alpha = \alpha_0 + \beta I + \gamma I^2$ , where  $\alpha_0$ ,  $\beta$  and  $\gamma$  are the linear absorption, TPA and fifth-order nonlinear absorption coefficients, respectively. It should be noted that  $\beta$  and  $\gamma$  are

independent of  $I$ . Both  $\beta$  and  $\gamma$  can be determined by the best fittings between the open-aperture Z-scans and the Z-scan theory of TPA induced ESA.<sup>47</sup> Through numerical simulation, we obtained the values of  $\beta$  and  $\gamma$  at multi-wavelengths. Using the value of TPA coefficient  $\beta$ , the TPA cross section  $\sigma_{TPA}$  was achieved by the definition of  $\sigma_{TPA} = h\nu\beta/N$ . All the open-aperture broadband Z-scan measurements of **P1** were shown in Fig. S6 (Supporting Information) and the values of  $\beta$ ,  $\gamma$  and  $\sigma_{TPA}$  at experimental wavelengths for **P1** were summarized in Table 2.

The similar analysis was applied to **P2** and Z-scan measurements of **P2** at multi-wavelengths were shown in Fig. S7 (Supporting Information). The values of  $\beta$ ,  $\gamma$  and  $\sigma_{TPA}$  at experimental wavelengths for **P2** were also summarized in Table 2.

From the Table 2, under every wavelength photoexcitation, both **P1** and **P2** experience both TPA and TPA induced ESA effect, demonstrating that they have broad spectral optical limiting characteristic. The measured  $\sigma_{TPA}$  values are comparable to the ones reported by Albota et al. for large TPA cross section of organic molecules.<sup>48</sup> According to our experimental results, due to higher average pyrene possession ratio occupied in frontier molecular orbitals, the parameters of TPA and TPA induced ESA of **P1** are larger than that of **P2**.

### 3.4 Optical limiting behavior

In Fig. 5(a), the variations of the normalized transmittance of **P1** in DMSO solution as a function of the laser input irradiance through a 5 mm spectroscopic quartz cuvette for 900 nm, 850 nm, 800 nm, 750 nm, 650 nm, 600 nm, 532 nm and 515 nm are shown. As can be seen, the normalized transmittance of **P1** solution decreases with

**Table 2.** The parameters of TPA and TPA induced ESA under different wavelengths achieved from open-aperture Z-scan measurements

Wavelength [nm]	<b>P1</b>			<b>P2</b>		
	$\beta$ [ $10^{-2}$ cm/GW]	$\sigma_{TPA}$ [ $10^{-50}$ cm <sup>4</sup> sphoton <sup>-1</sup> ]	$\gamma$ [ $10^{-4}$ cm <sup>3</sup> /GW <sup>2</sup> ]	$\beta$ [ $10^{-2}$ cm/GW]	$\sigma_{TPA}$ [ $10^{-50}$ cm <sup>4</sup> sphoton <sup>-1</sup> ]	$\gamma$ [ $10^{-4}$ cm <sup>3</sup> /GW <sup>2</sup> ]
900	0.40±0.05	10.7±1.3	6.0±0.4	-	-	-
850	0.50±0.01	14.2±0.3	4.5±0.2	-	-	-
800	0.45±0.07	13.6±2.1	3.8±0.5	0.16±0.02	4.8±0.6	1.5±0.4
750	0.43±0.03	13.8±1.0	3.1±0.5	0.20±0.04	6.4±0.9	3.0±0.2
650	1.2±0.1	44.5±3.7	9.7±1.5	0.50±0.10	18.5±1.7	2.0±0.5
600	2.0±0.2	80.3±8.0	21.2±1.9	0.60±0.10	24.1±2.2	3.8±0.3
532	3.8±0.6	172±27	43.8±2.2	1.0±0.1	45.3±2.4	9.2±1.2
515	8.5±0.8	394±18	56.5±6.5	-	-	-

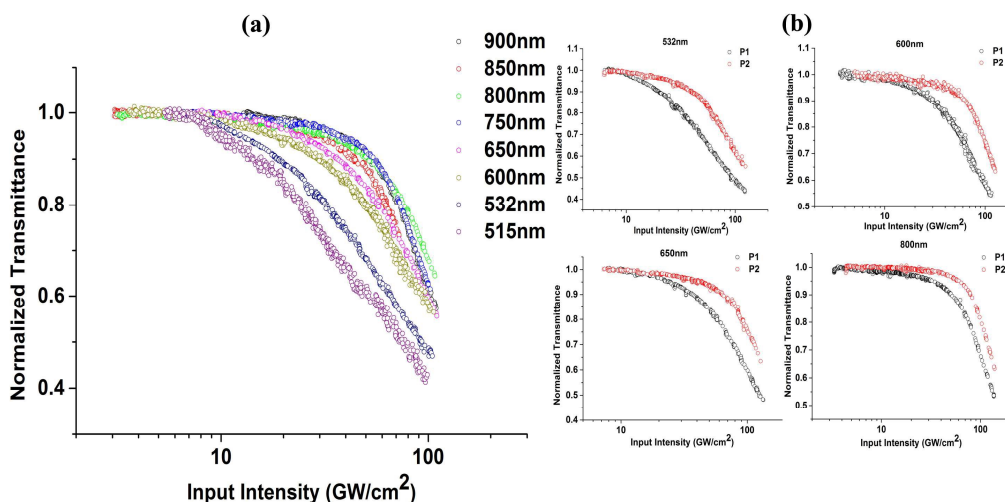


**Fig. 5** (a) Ultrafast optical limiting of **P1** as a function of the input irradiance at 900 nm, 850 nm, 800 nm, 750 nm, 650 nm, 600 nm, 532 nm and 515 nm with 190 fs excitation. (b) comparison of optical limiting for **P1** and **P2** at 532 nm, 600 nm, 650 nm and 800 nm

increasing input irradiance under multi-wavelengths excitation, exhibiting excellent broadband optical limiting performance range from 515 nm to 900 nm for femtosecond laser pulses. Through previous meticulous analysis, the mechanism for optical limiting under multi-wavelengths is attributed to TPA and TPA induced ESA. Due to larger parameters of TPA and TPA induced ESA, the optical limiting behavior of **P1** is obvious better than that of **P2** at multi-wavelengths, shown in Fig. 5(b). As Fig. 5(a) is shown, **P1** exhibit nearly 40% modulation in the normalized transmittance at 100 GW/cm<sup>2</sup> under multi-wavelengths. Optical limiting performances of **P1** with femtosecond laser pulses is comparable or better than previous reported Fe<sub>3</sub>O<sub>4</sub> nanocomposite,<sup>49, 50</sup> organic molecular nano/microcrystals,<sup>51</sup> calixarenes<sup>52</sup> and Coumarin-120,<sup>31</sup> indicating pyrene-based materials as potential ultrafast broadband optical limiters.

#### 4. Conclusions

In summary, we have prepared two novel isomeric molecules based on pyrene for ultrafast broadband optical limiters. The NLO properties of materials can be improved by modifying main nonlinear group possession ratio occupied in frontier molecular orbitals. Due to higher average pyrene possession ratio occupied in frontier molecular orbitals, **P1** performed better NLO properties than **P2**, which was consistent with the experimental results. Excellent optical limiting behaviors were observed under femtosecond laser excitations at multi-wavelengths (range from 515 to 900 nm), which resulted from TPA and TPA induced ESA. Moreover, **P1** was extremely high transmittance (> 91%) from visible to infrared regions (500 to 900 nm). The fascinating properties of pyrene-based derivative such as low cost, simple synthesis procedure and excellent broadband NLO properties make it a promising candidate for broadband ultrafast optical limiters.

#### Acknowledgements

The authors gratefully acknowledge the support of the National Natural Science Fund of China (Grant No. 11304216) and we are grateful to Prof. Li Jiang for structural characterization (<sup>1</sup>H NMR, <sup>13</sup>C NMR and MALDI-TOF mass spectrosopes) of these two samples.

#### Notes and references

1. K. M. Nashold, D. P. Walter, *J. Opt. Soc. Am. B* 1995, 12, 1228-1237.
2. K. Mansour, M. Soileau, E. W. Van Stryland, *J. Opt. Soc. Am. B* 1992, 9, 1100-1109.
3. G.-K. Lim, Z.-L. Chen, J. Clark, R. G. S. Goh, W.-H. Ng, H.-W. Tan, R. H. Friend, P. K. H. Ho, L.-L. Chua, *Nat. Photonics* 2011, 5, 554-560.
4. M. Feng, H. Zhan, Y. Chen, *Appl. Phys. Lett.* 2010, 96.
5. J. Wang, Y. Hernandez, M. Lotya, J. N. Coleman, W. J. Blau, *Adv. Mater.* 2009, 21, 2430.
6. J. E. Riggs, D. B. Walker, D. L. Carroll, Y.-P. Sun, *J. Phys. Chem. B* 2000, 104, 7071-7076.
7. L. Vivien, E. Anglaret, D. Riehl, F. Bacou, C. Journet, C. Goze, M. Andrieux, M. Brunet, F. Lafonta, P. Bernier, *Chem. Phys. Lett.* 1999, 307, 317-319.
8. P. Chen, X. Wu, X. Sun, J. Lin, W. Ji, K. Tan, *Phys. Rev. Lett.* 1999, 82, 2548.
9. L. W. Tutt, A. Kost, *Nature* 1992, 356, 225.
10. S. M. O'Flaherty, S. V. Hold, M. J. Cook, T. Torres, Y. Chen, M. Hanack, W. J. Blau, *Adv. Mater.* 2003, 15, 19.
11. J. Perry, K. Mansour, I.-Y. Lee, X.-L. Wu, P. Bedworth, C.-T. Chen, D. Ng, S. Marder, P. Miles, T. Wada, *Science* 1996, 273, 1533-1536.
12. M. O. Senge, M. Fazekas, E. G. Notaras, W. J. Blau, M. Zawadzka, O. B. Locos, E. M. Ni Mhuircheartaigh, *Adv. Mater.* 2007, 19, 2737-2774.
13. M. Calvete, G. Y. Yang, M. Hanack, *Synthetic Met.* 2004, 141, 231-243.
14. Z. Qin, J. C. Bischof, *Chem. Soc. Rev.* 2012, 41, 1191-1217.

15. L. Vivien, D. Riehl, J.-F. Delouis, J. A. Delaire, F. Hache, E. Anglaret, *J. Opt. Soc. Am. B* 2002, 19, 208-214.
16. L. Vivien, D. Riehl, E. Anglaret, F. Hache, *IEEE J. Quantum Elect.* 2000, 36, 680-686.
17. Y. Xiong, L. Yan, J. Si, W. Yi, W. Ding, W. Tan, X. Liu, F. Chen, X. Hou, *J. Appl. Phys.* 2014, 115, 083111.
18. N. Liaros, E. Koudoumas, S. Couris, *Appl. Phys. Lett.* 2014, 104, 19112.
19. D. Chateau, Q. Bellier, F. Chaput, P. Feneyrou, G. Berginc, O. Maury, C. Andraud, S. Parola, *J. Mater. Chem. C* 2014, 2, 5105-5110.
20. S. Husaini, J. E. Slagle, J. M. Murray, S. Guha, L. P. Gonzalez, R. G. Bedford, *Appl. Phys. Lett.* 2013, 102, 191112.
21. Z. Yang, Z. K. Wu, J. S. Ma, A. D. Xia, Q. S. Li, C. L. Liu, Q. H. Gong, *Appl. Phys. Lett.* 2005, 86, 061903.
22. Q. S. Li, C. L. Liu, Z. G. Liu, Q. H. Gong, *Opt. Express* 2005, 13, 1833-1838.
23. C. Li, C. L. Liu, Q. S. Li, Q. H. Gong, *Chem. Phys. Lett.* 2004, 400, 569-572.
24. J. Staromlynska, T. J. McKay, P. Wilson, *J. Appl. Phys.* 2000, 88, 1726-1732.
25. J. S. Shirk, R. G. S. Pong, S. R. Flom, H. Heckmann, M. Hanack, *J. Phys. Chem. A* 2000, 104, 1438-1449.
26. M. Cha, N. S. Sariciftci, A. J. Heeger, J. C. Hummelen, F. Wudl, *Appl. Phys. Lett.* 1995, 67, 3850-3852.
27. G.-J. Zhou and W.-Y. Wong, *Chem. Soc. Rev.* 2011, 40, 2541-2566.
28. G. Zhou, W. Y. Wong, S. Y. Poon, C. Ye and Z. Lin, *Adv. Funct. Mater.* 2009, 19, 531-544.
29. G. J. Zhou, W. Y. Wong, C. Ye and Z. Lin, *Adv. Funct. Mater.* 2007, 17, 963-975.
30. G.-J. Zhou, W.-Y. Wong, D. Cui and C. Ye, *Chem. Mater.* 2005, 17, 5209-5217.
31. B. Anand, N. Roy, S. S. S. Sai, R. Philip, *Appl. Phys. Lett.* 2013, 102, 203302.
32. X.-F. Jiang, L. Polavarapu, S. T. Neo, T. Venkatesan, Q.-H. Xu, *J. Phys. Chem. Lett.* 2012, 3, 785-790.
33. Q. Zheng, G. S. He, P. N. Prasad, *Chem. Phys. Lett.* 2009, 475, 250-255.
34. J. M. Hales, M. Cozzuol, T. E. O. Screen, H. L. Anderson, J. W. Perry, *Opt. Express* 2009, 17, 18478-18488.
35. S.-H. Chi, J. M. Hales, M. Cozzuol, C. Ochoa, M. Fitzpatrick, J. W. Perry, *Opt. Express* 2009, 17, 22062-22072.
36. C. L. Devi, K. Yesudas, N. S. Makarov, V. J. Rao, K. Bhanuprakash, J. W. Perry, *J. Mater. Chem. C* 2015, 3, 3730-3744.
37. H. M. Kim, Y. O. Lee, C. S. Lim, J. S. Kim, B. R. Cho, *J. Org. Chem.* 2008, 73, 5127-5130.
38. H. S. Nalwa, *Adv. Mater.* 1993, 5, 341-358.
39. C. V. Francis, K. M. White, G. T. Boyd, R. S. Moshrefzadeh, S. K. Mohapatra, M. D. Radcliffe, J. E. Trend, R. C. Williams, *Chem. Mater.* 1993, 5, 506-510.
40. H. Hou, Y. Wei, Y. Song, L. Mi, M. Tang, L. Li, Y. Fan, *Angewandte Chemie* 2005, 117, 6221-6228.
41. M. J. Frisch, G. W. Trucks, H. B. Schlegel, G. E. Scuseria, M. A. Robb, J. R. Cheeseman, G. Scalmani, V. Barone, B. Mennucci, G. A. Petersson, H. Nakatsuji, M. Caricato, X. Li, H. P. Hratchian, A. F. Izmaylov, J. Bloino, G. Zheng, J. L. Sonnenberg, M. Hada, M. Ehara, K. Toyota, R. Fukuda, J. Hasegawa, M. Ishida, T. Nakajima, Y. Honda, O. Kitao, H. Nakai, T. Vreven, J. A. Montgomery, J. E. Peralta, F. Ogliaro, M. Bearpark, J. J. Heyd, E. Brothers, K. N. Kudin, V. N. Staroverov, R. Kobayashi, J. Normand, K. Raghavachari, A. Rendell, J. C. Burant, S. S. Iyengar, J. Tomasi, M. Cossi, N. Rega, J. M. Millam, M. Klene, J. E. Knox, J. B. Cross, V. Bakken, C. Adamo, J. Jaramillo, R. Gomperts, R. E. Stratmann, O. Yazyev, A. J. Austin, R. Cammi, C. Pomelli, J. W. Ochterski, R. L. Martin, K. Morokuma, V. G. Zakrzewski, G. A. Voth, P. Salvador, J. J. Dannenberg, S. Dapprich, A. D. Daniels, O. Farkas, J. B. Foresman, J. Ortiz, V. J. Cioslowski, and D. J. Fox, *Gaussian 09, Revision A.01*, Gaussian, Inc., Wallingford CT, 2009.
42. N.M. O'Boyle, A.L. Tenderholt and K.M. Langner, *J. Comp. Chem.* 2008, 29, 839-845.
43. M. Sheik-Bahae, A. A. Said, T.-H. Wei, D. J. Hagan, E. W. Van Stryland, *IEEE J. Quantum Elect.* 1990, 26, 760-769.
44. R. L. Sutherland, M. C. Brant, J. Heinrichs, J. E. Rogers, J. E. Slagle, D. G. McLean, P. A. Fleitz, *J. Opt. Soc. Am. B* 2005, 22, 1939-1948.
45. S. Delysse, P. Filloux, V. Dumarcher, C. Fiorini, J.-M. Nunzi, *Opt. Mater.* 1998, 9, 347-351.
46. T. Xia, A. Dogariu, K. Mansour, D. Hagan, A. Said, E. Van Stryland, S. Shi, *J. Opt. Soc. Am. B* 1998, 15, 1497-1501.
47. B. Gu, W. Ji, P. Patil, S. Dharmaparakash, H.-T. Wang, *Appl. Phys. Lett.* 2008, 92, 091118-091113.
48. M. Albota, D. Beljonne, J.-L. Brédas, J. E. Ehrlich, J.-Y. Fu, A. A. Heikal, S. E. Hess, T. Kogej, M. D. Levin, S. R. Marder, D. McCord-Maughon, J. W. Perry, H. Röckel, M. Rumi, G. Subramaniam, W. W. Webb, X.-L. Wu, C. Xu, *Science* 1998, 281, 1653-1656.
49. P. Thomas, P. Sreekanth and K. E. Abraham, *J. Appl. Phys.* 2015, 117, 053103.
50. G. Xing, J. Jiang, J. Y. Ying and W. Ji, *Opt. Express* 2010, 18, 6183-6190.
51. A. Patra, N. Venkatram, D. N. Rao and T. Radhakrishnan, *J. Phys. Chem. B* 2008, 112, 16269-16274.
52. C. P. Singh, R. Sharma, V. Shukla, P. Khundrakpam, R. Misra, K. S. Bindra and R. Chari, *Chem. Phys. Lett.* 2014, 616, 189-195.